International Journal of Basic and Applied Sciences, 14 (4) (2025) 675-684

International Journal of Basic and Applied Sciences

Website: www.sciencepubco.com/index.php/IJBAS
https://doi.org/10.14419/3v49kz60
Research paper

Hybrid Cascaded ANFIS-RNN-Based MPPT Controller For PV-Driven Grid System

Blessy A. Rahiman [1] *, J. Jayakumar [1], R. Meenal [2]

[1] Department of Electrical and Electronics Engineering, Karunya Institute of Technology and Sciences, Coimbatore, India
[2] Department of Electrical and Electronics Engineering, SRM TRP Engineering College, Trichy - 621105, India
**Corresponding author E-mail: blessynaz@gmail.com*

Received: July 7, 2025, Accepted: August 13, 2025, Published: August 27, 2025

Abstract

The clean energy aspect of solar Photovoltaic (PV) energy is becoming more popular in today's distribution networks, and the solar modules' output power is nonlinear owing to atmospheric conditions. To maximize the power generation from PV systems, efficient Maximum Power Point Tracking (MPPT) techniques and voltage regulation are crucial. Therefore, the proposed work incorporated the hybrid Cascaded Adaptive Network-Based Fuzzy Inference System (ANFIS) - Recurrent Neural Network (RNN) based MPPT and boost converter system for PV-tied grid systems. The proposed Boost converters are used to convert the PV panels' changing DC voltage into a stable and suitable voltage level for grid integration with high efficiency and low THD. Furthermore, to track optimal power from the PV system, cascaded ANFIS-RNN is employed. The cascaded ANFIS controller provides a robust and adaptive approach for tracking the Maximum Power Point (MPP), ensuring optimal extraction of power from PV panels, and to further enhance the MPPT performance, an RNN is integrated into the ANFIS controller, which leads to increased tracking precision and quicker convergence. The single-phase VSI is used to convert DC-AC supply for distributing power to the grid system, and it is controlled with the aid of PI controller. Finally, MATLAB/Simulink is used to implement the entire proposed concept, and a comparative analysis is made over with the existing topologies to prove the prominence of the developed work.

Keywords: *ANFIS-RNN; MATLAB/Simulink; MPPT; Photovoltaic; PI controller; Single Phase VSI.*

1. Introduction

Depleting fossil fuel reserves and escalating environmental concerns are the main drivers of the global switch from alternative energy sources to those reliant on fossil fuels. Nearly all nations worldwide are dedicated to using renewable energy sources to cut down on greenhouse gas emissions in place of conventional fossil fuels. Among these, photovoltaic (PV) energy has emerged as a leading choice [1-3]. With the increasing demand for electricity and the gradual phasing out of conventional thermal power plants fuelled by coal and other fossil fuels, renewable energy sources are gaining popularity for generating power. Solar photovoltaic systems are particularly crucial for power generation due to their cost-effectiveness, quiet operation, and straightforward design. From low-power to high-power grid systems, solar PV power generation has been effectively migrated [4], [5].

In general, DC-DC converters come in two primary varieties: distinct and non-distinct, respectively. An electric barrier is created by a high-frequency transformer between the former's input and output, but the latter lacks one entirely. To safeguard the delicate loads connected to the converter, the electric barrier is primarily used. Yet, Non-isolated DC-DC converters achieve increased efficiency in addition to lower cost and space since they do not have an electric barrier in their structure [6], [7]. To overcome the drawbacks of these converters, this work focuses on an output voltage that is higher due to an input boost converter, ideal for situations requiring a higher voltage from a lower input source.

As an alternative, improving the control strategies of current systems for better MPPT is a simple and affordable solution. This leads to an instantaneous boost in power generation, hence reducing overall expenses. These methodologies employ diverse search strategies to provide a range of PV system applications [8]. These MPPT techniques fall into three general categories: computation, artificial intelligence, and hill-climbing. The notion of hill-climbing is fundamental to techniques like IC and P&O. It involves identifying direction in power development and adjusting the PV panel's operating point to align with that direction. However, because of their continual oscillation around MPP, these techniques cause a loss of PV production in scenarios with gradual variations in environmental conditions [9]. As artificial intelligence tools have developed, multiple iterations of control schemes for PV system MPPTs have been introduced. Effective MPPT is commonly achieved using ANN and fuzzy logic control, which are dependable, accurate, and quick [10], [11], but they are complex and sensitive to parameter settings.

Recent MPPT approaches like Radial Basis Function Neural Network (RBFNN) [12], Artificial Neural Network [13], [14], ANFIS [15] are adopted for efficient power utilization. Anyway, improper training or overfitting can cause poor generalization under unfamiliar weather

conditions. Their design, parameter tuning, and training phases are time-consuming, and they may require periodic retraining to maintain accuracy over the system's lifetime. This work introduces Hybrid Cascaded ANFIS-RNN-MPPT, a Hybrid MPPT approach blending multiple algorithms to enhance tracking efficiency and resilience, albeit with increased complexity and tuning requirements.
By implementing a Cascaded ANFIS-RNN MPPT controller, this work aims to enhance MPPT efficiency and accuracy, improve resilience against environmental fluctuations, and reduce steady-state error in photovoltaic (PV) systems for optimized energy harvesting. The following defines the main contributions:

- PV systems use a hybrid strategy that combines many controllers and algorithms to optimize energy gathering efficiency.
- The Boost converter addresses the limitations of step-down converters by increasing voltage efficiently.
- The use of a PI controller with a Hybrid cascaded ANFIS-RNN-based MPPT for PI controller in PV systems is proposed for enhanced efficiency, accuracy, and resilience.

2. Proposed methodology

The integration of a photovoltaic (PV) system with various components aims to optimize energy conversion efficiency and enhance system performance. The process begins with an effective Boost Converter that increases the voltage the photovoltaic system generates. This higher voltage is then fed into a Voltage Source Inverter (VSI) that operates on a single phase, converting DC voltage to AC, making it suitable for grid integration. Control of the VSI output is achieved through Pulse Width Modulation (PWM) done by a dedicated PWM Generator. These pulses regulate the VSI output, ensuring that it meets power references for reactive (Q_{ref}) and active (P_{ref})power. To further refine VSI output and ensure its compatibility with the grid, the LC Filter is used to reduce any variations in power. The single-phase electrical grid is connected to the system, with actual power values and voltage, current measurements monitored at the PV system for performance evaluation and control purposes. Figure 1 displays the Architecture of the proposed description.

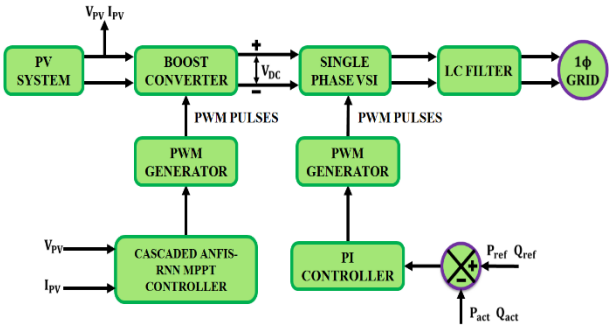

Fig. 1: Architecture of the Proposed Description.

The standout feature of this methodology is the Hybrid Cascaded ANFIS-RNN MPPT Controller. This controller's purpose is to continuously monitor the PV system's MPP, thereby maximizing its energy conversion efficiency. The controller uses the ANFIS-MPPT algorithm to dynamically modify the PV system's operating parameters based on the fuzzy rules combined with neural network learning. Additionally, the controller employs an RNN architecture, which is well-suited for processing sequential data such as measuring time series from the PV system. This combination of optimization algorithm and neural network architecture enables the controller to adapt to changing environmental conditions and rapidly respond to fluctuations in solar irradiance, ensuring optimal PV system performance under various operating circumstances. Overall, the proposed methodology represents a comprehensive approach to integrating a PV system with advanced control and optimization techniques. By leveraging the unique capabilities of the Hybrid Cascaded ANFIS-RNN MPPT Controller, the system achieves higher energy conversion efficiency and improved performance.

3. System modelling

3.1. Modelling of PV system

PV panels [3] are composed of PV cells linked either in series or parallel. As shown in Figure 2, a single diode model is used to illustrate the mathematical representation of a PV array to represent a PV cell.

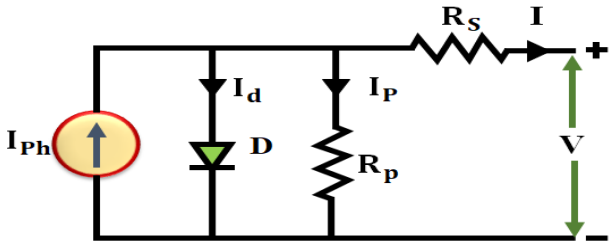

Fig. 2: Modelling of PV System.

The following are the mathematical formulas used to represent PV panels with a number of series cells(N_s).

$$I = I_{ph} - I_s\left(\exp\left(\frac{V+IR_s}{aN_sV_t}\right) - 1\right) - \frac{V+IR_s}{R_p} \quad (1)$$

$$V_t = \frac{kT_C}{q} \quad (2)$$

$$I_{ph} = \frac{G}{G_n}\left(I_{sc_n} + K_I\left(T_C - T_{C_n}\right)\right) \quad (3)$$

$$I_s = I_{S_n}\left(\frac{T_C}{T_{C_n}}\right)\exp\left(\frac{qE_g}{ak}\left(1/T_{C_n} - 1/T_C\right)\right) \quad (4)$$

$$I_{S_n} = I_{Sc_n}/\left(\exp\left(\frac{V_{Oc_n}}{aN_sV_{t_n}}\right) - 1\right) \quad (5)$$

The photocurrent $(I_{ph})$of the photovoltaic panel is the saturation current; the thermal voltageV_t, solar irradiationG, cell temperatureT_C, band gap$E_g$of the semiconductor material, Boltzmann constant k, electron charge q, and ideality factor (a). There is also the open circuit voltage V_{oc} and the short circuit currentI_{sc}. The number of parallel strings(N_{P_s}), number of series panels(N_{S_p}), series resistance(R_s), and parallel resistance(R_p) are interchangeable. With the use of a converter, photovoltaic (PV) energy has the benefit of directly converting sunlight into electrical power, making it a sustainable, efficient, and environmentally beneficial power source.

3.2. Design of boost converter

Switch converters must be connected to a resistive load and a PV panel to ensure the optimal power operating point. The operation of a boost converter is to raise the input voltage to a regulated output [16]. The power conversion can operate in two distinct scenarios based on the inductor I_L current. If I_L does not equal zero, the continuous conduction mode (CCM) commences. The output current I_o falls below the maximum CCM switching limit, or frequency lowers, causing irregular conduction mode (DCM).
Figure 3 shows the typical structure of the CCM-functioning converter.

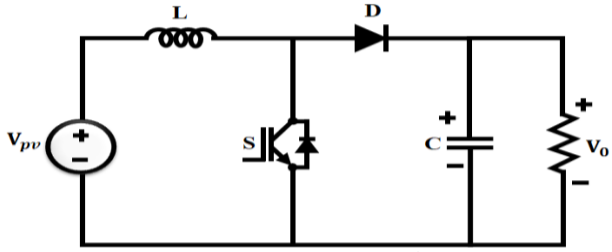

Fig. 3: Boost Converter Topology.

The booster converter's state space depiction, a nonlinear system with a variable structure, is defined as follows:

$$\begin{bmatrix}\dot{I_L}\\ \dot{V_o}\end{bmatrix} = \begin{bmatrix}0 & \frac{\alpha-1}{L}\\ \frac{1-\alpha}{C} & \frac{1}{R_oc}\end{bmatrix}\begin{bmatrix}I_L\\ V_O\end{bmatrix} + \begin{bmatrix}\frac{1}{L}\\ 0\end{bmatrix}v \quad (6)$$

The bilinear model could be used to enable the system: $\dot{x} = f(x) + g(x)u$

$$\begin{bmatrix}\dot{I_L}\\ \dot{V_o}\end{bmatrix} = \begin{bmatrix}\frac{V_{pv}}{L} - & \frac{V_O}{L}\\ \frac{I_L}{C} + & \frac{V_O}{R_OC}\end{bmatrix} + \begin{bmatrix}\frac{V_O}{L}\\ -\frac{I_L}{C}\end{bmatrix}\alpha \quad (7)$$

Where,

$$f(x) = \begin{bmatrix}\frac{1}{L} & \left(V_{pv} - V_O\right)\\ \frac{1}{C} & \left(I_L - \frac{V_O}{R_O}\right)\end{bmatrix}, g(x) = \begin{bmatrix}\frac{V_O}{L}\\ -\frac{I_L}{C}\end{bmatrix} \text{and } u = \alpha \quad (8)$$

The duty ratio (α) directly relates to the relationship between the voltages of the input and output.

$$V_O = \frac{V_{pv}}{1-\alpha} \quad (9)$$

The solar module's power supply and the load's power delivery must be equal, assuming that there is no loss $P_{pv} = P_0$.

$$P_{pv} = P_0 \Rightarrow V_{pv}I_{pv} = V_OI_O \quad (10)$$

Equation (10) is substituted into Equation (9) to produce:

$$I_O = I_{pv}(1-\alpha) \quad (11)$$

$R_O = V_O/I_O$The resistance load gives us:

$$R_O = \frac{R_{pv}}{(1-\alpha)^2} \quad (12)$$

The benefit of utilizing a boost converter in MPPT is that it effectively increases the input voltage, guaranteeing that the solar system maximizes its power under a range of circumstances and maximizing energy harvesting.

3.3. Cascaded ANFIS algorithm

The hybrid algorithm ANFIS blends fuzzy logic (FL) with neural networks (NNs) [17], combining their strengths. Its six-layer structure includes an input layer, a layer for FL-based membership function construction, and a cumulative generation layer. Subsequent layers are applied before reaching the final layer for result production. ANFIS processes absolute values, converting them into fuzzy values, which are then used in fuzzy reasoning. Afterward, these fuzzy values are transformed into crisp values. This repeatable implementation, illustrated in Figure 4, utilizes one output and two major inputs. Iterations enhance accuracy, making it a valuable addition to the traditional five-layer ANFIS algorithm.

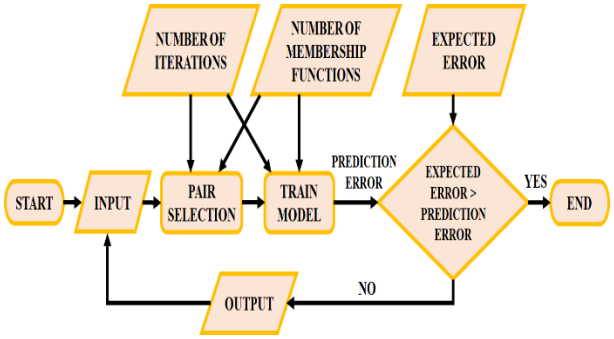

Fig. 4: The Cascaded ANFIS Flowchart.

The cascaded ANFIS algorithm is distinct from the standard ANFIS algorithm in that its output is designed for future use as input for the standard ANFIS. Fuzzification, akin to the conventional ANFIS, takes place within the internal layers, transforming numerical values into fuzzy members using membership functions. Cascaded ANFIS consists of a training approach and a pair selection mechanism, addressing a significant issue of ANFIS by leveraging all features to construct a robust model suitable for noisy datasets. The computational complexity of training the innovative Cascaded ANFIS algorithm is managed by the pair selection module, which uses sequential feature selection to choose candidates. This method generates current outputs and root mean square error (RMSE) for specific data combinations. This RMSE is compared to the desired error, set as the goal error, and the process concludes when the target error is reached. The second level then utilizes those outputs as inputs to itself to initialize.

$$f = \frac{\sum_{j=1}^{6} O_{n,j}}{6} \tag{13}$$

The optimal ANFIS at the second level in a pair is chosen once more through the pair selection procedure. This procedure continues until the predetermined maximum level is attained. Equation (17) finds the final value f by averaging the outputs at the end. In this case, the output at n of the jth The ANFIS module is $O_{n,j}$. The ability to combine the adaptive learning and inference capabilities of ANFIS with the sequential and memory-retention properties of RNNs is the benefit of using cascaded ANFIS with RNN, improving the system's performance in dynamic and challenging environments involving time-series predictions.

3.4. RNN-based MPPT

PV module voltage and current are adjusted by the MPPT [18], and the resultant voltage and current are maximum. Use the following formula to determine the duty cycle D, which combines the voltage error and reference signal:

$$V_{error} = V_{MPP(STC)} - V_{pv} \tag{14}$$

The PV module temperature (T) is used in the temperature gradient approach to alter$V_{MPP(STC)}$, based on the temperature/voltage coefficientβ. Different modules have different coefficients of βvalue.

$$V_{pv} = V_{MPP(STC)} + \beta(T_{ref} - T) \tag{15}$$

Given that the temperature and irradiance in the current are represented as follows,

$$I = \left\{\left[I_{SC_{ref}} + a(T_{ref} - T)\right] \cdot \frac{S}{S_{ref}}\right\} - I_D \cdot \left(e^{q\left(\frac{(V+I.R_s)}{\eta}.K.T\right)} - 1\right) - \frac{V+I.R_s}{R_p} \tag{16}$$

Reference irradiance is represented by the symbolS_{ref}, the measured irradiance by the symbolS, and the temperature-dependent current sensitivity is given by the symbol a. The behavior, where temperature and irradiance directly affect, is modeled using the solar module Equation (16). Irradiance rises together with PV power. It is possible to assess the MPP's variables using observed equations and traits. Numerous constraints exist, such as a high number of modules, high cost, and low power. To improve the MPP, a novel and straightforward technique is implemented.

In contrast to feed-forward neural networks, RNNs are much more powerful. The symbols X, , and Z stand for the input, output, and hidden vectors, respectively. The letter H represents the hidden vector. RNN-dependent MPPT governs the PV technique. Duty cycle (D), the output that controls how well the converter works, is regulated by temperature (T) and radiation (G), the meteorological data utilized as input variables for Maximum Power Point Tracking (MPPT).

$X = (x_1, x_2, \cdots, x_T)$ is the input vector sequence, $H = (h_1, h_2, \cdots, h_T)$hidden vector sequence, and $Y = (y_1, y_2, \cdots, y_T)$is the output vector sequence. These values are computed with $t = 1$ to tas below:

$$h_t = \sigma(W_{xh}X_t + W_{hh}h_{t-1} + b_h) \quad (17)$$

$$y_t = W_{hy}h_t + b_y \quad (18)$$

While $Wandb, h_{t-1}$ represents weight and bias and σ represents the nonlinearity activation function,
RNN has certain problems with the local optimum, which disappears when the gradient function is trained using BPTT. Using the long short-term memory (LSTM) in the RNN, the time series is classified order get around the problem of local optima.
An LSTM is made up of cell states and one LSTM cell. In the LSTM, three gates are denoted as i, f, o adjust the data. First, the input gate and candidate value are computed in relation to timet, as stated below.

$$i_t = \sigma(W_{Xi}X_t + W_{hi}h_{t-1} + W_{Ci}C_{t-1} +)b_i \quad (19)$$

$$C_t = f_tC_{t-1} + i_C \tan h\,(W_{Xc}X_t + W_ch_{t-1} + b_c) \quad (20)$$

The forget gates decide if using Equation (20) to transmit the memory toh_{t-1}

$$f_t = \sigma(W_{Xf}X_t + W_{hf}h_{t-1} + W_{cf}C_{t-1} + b_f) \quad (21)$$

The output gates use Equation (21) to determine whether to pass the output of the memory cell.
Equation (22) illustrates this procedure.

$$O_t = \sigma(W_{Xo}X_t + W_{ho}h_{t-1} + W_{co}C_t + b_o) \quad (22)$$

$$h_t = O_t \tan h\,(C_t) \quad (23)$$

The above expressions indicate that the representation of the weight matrices functions asW_{Ci}, W_{Cf}andW_{Co}; the memory cell layer's input is represented as X_t at timet, the input gate is called asi, the forget gate is called asf, the output is calledo, and the cell state is calledc. RNN-based MPPT controllers benefit from the Cascaded ANFIS algorithm because it optimizes the RNN's parameters to improve tracking performance in PV systems, hence raising the MPPT method's efficiency and accuracy.

3.5. PI controller

Among the controllers that are used in practical applications, the most common is the PI controller. Figure 5 depicts the block PI [19] controller schematic diagram.

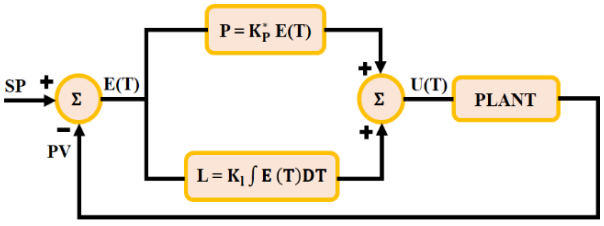

Fig. 5: Block Diagram of PI Controller.

The proportionate part and the integral part are its two constituent parts. Eliminating the integral component aims to detect the steady state inaccuracy. As seen by$u(t)$The time domain output of the PI controller corresponds to the plant's control input.
Equation 24provides a calculation given by,

$$u(t) = K_p e(t) + K_I \int e(t)dt \quad (24)$$

Where, K_pGain proportional,$K_I$integral gain factor, $e(t)$error. K_p be found using Equation 25.

$$K_I = \frac{K_p}{T_i} \quad (25)$$

The following equation results from substituting (24) into (25):

$$u(t) = K_p(e(t) + \frac{1}{T_i}\int e(t)dt \quad (26)$$

Where the time is reset toT_i. T_i and K_p These are tuning parameters. The benefit of employing a PI controller in grid voltage synchronization is its capacity to accurately and steadily control voltage error, guaranteeing accurate and stable synchronization of the renewable energy system and grid.

4. Results and discussion

A detailed review of the proposed approach, which employs an RNN MPPT system optimized for Cascaded ANFIS and a Boost converter output, will be covered in this part. Important metrics, including voltage stability, converter efficiency, and the overall efficacy of the optimized control method, will also be covered. This paper examined a novel approach: using a PI controller to maximize performance in a1ϕVSI. Using MATLAB, the efficiency of a certain system is evaluated, and its full simulation is verified.

Table 1: Parameter Specification

Parameter	Rating
Solar PV System	
Short Circuit Current	8.95A
Open Circuit Voltage	37.25V
Maximum Peak Voltage	29.95V
Total Power	10KW
Maximum Peak Current	8.35A
Peak Power	150W
Boost Converter	
L	1mH
C	3500μF
Switch	10kHz

Fig. 6: Solar Panel Temperature and Irradiation Waveform at Constant Scenario.

In the given Figure 6, the temperature stabilizes at$35^{\circ}\mathrm{C}$, indicating a consistent and constant temperature level. Concurrently, the irradiation stabilizes at$1000(\mathrm{w/sq.m})$, showing a consistent and stable level of solar irradiation.

Fig. 7: Voltage and Current in Solar Panels at Constant Scenario.

In Figure 7 provided, the voltage stabilizes at 250V, indicating a consistent and steady voltage level. Additionally, the current waveform stabilizes at 33.09A, observed at 0.3S, signifying a stable and constant current flow.

Fig. 8: Temperature and Irradiation Waveform of Solar Panel at Varying Scenario.

In the provided Figure 8, the temperature initially rises from $25^{\circ}\mathrm{C}$ and stabilizes at $35^{\circ}\mathrm{C}$ by the 0.3S, indicating a gradual increase followed by a steady state. Concurrently, the current waveform displays a value of 1000A at the same 0.3S, indicating a consistent and significant flow of electrical current at that specific point in time.

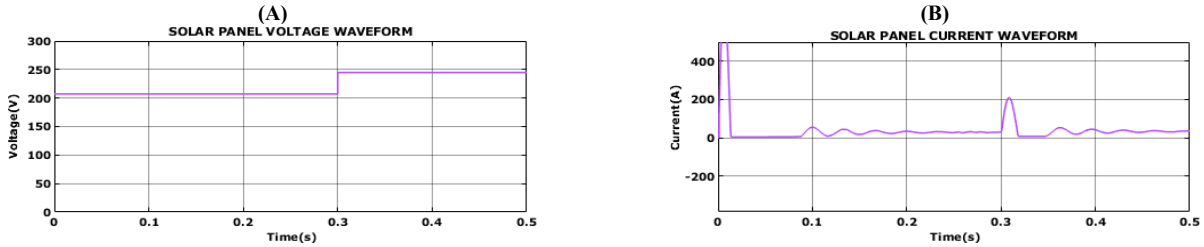

Fig. 9: The Solar Panel's Voltage and Current Waveform at Varying Scenario.

In Figure 9, the voltage stabilizes at 250V precisely at 0.3S, indicating a consistent and unwavering voltage level at that instance. Meanwhile, the current remains constant throughout, maintaining a value of 33.09A, signifying a steady and continuous flow of electrical current. Similarly, Figure 10 indicates a constant temperature at 35˚C and varying irradiation from 800 to 1000 W/sq.m.

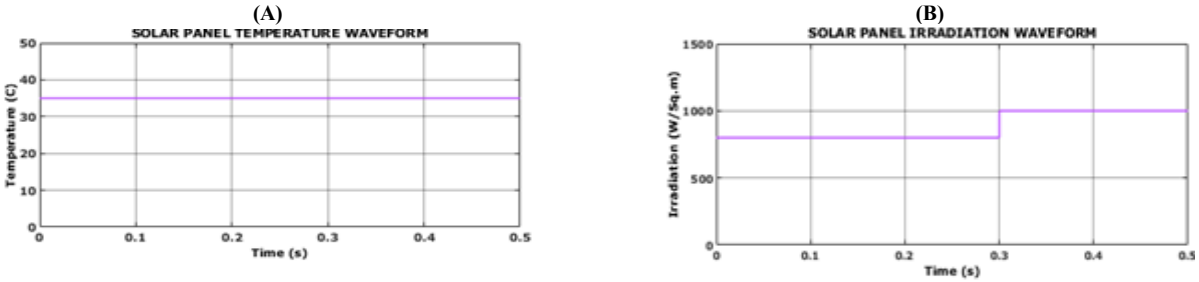

Fig. 10: Temperature And Irradiation Waveform at Constant Temperature and Varying Irradiation.

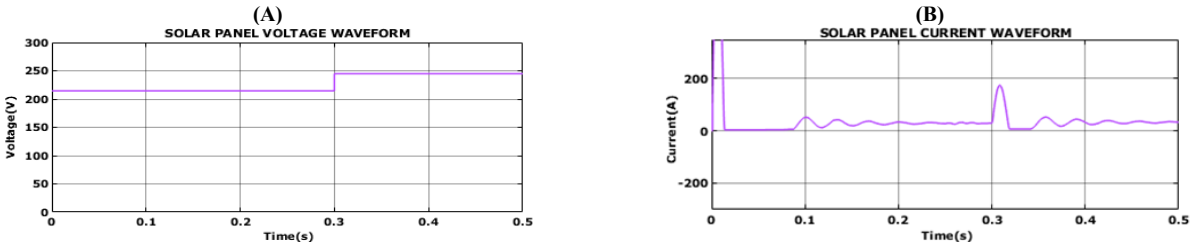

Fig. 11: Waveform of Solar Panel Voltage and Current at Varying and Constant Scenario.

In waveform 11, the voltage stabilizes at 250V exactly at 0.3s, showing a consistent and steady voltage level at that specific moment. Simultaneously, the current remains constant at 33.09A, indicating a stable and continuous flow of electrical current.

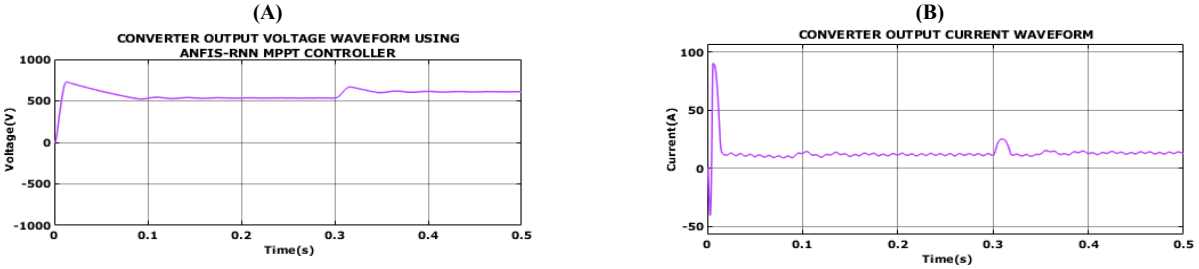

Fig. 12: Waveform of Converter Output Voltage and Current Under All Scenarios.

Under all cases, the voltage stabilizes at 600V precisely at 0.3s, indicating a consistent and steady voltage level as in Figure 12. Similarly, the current waveform stays constant at 12.47A, ensuring a stable and uninterrupted flow of current.

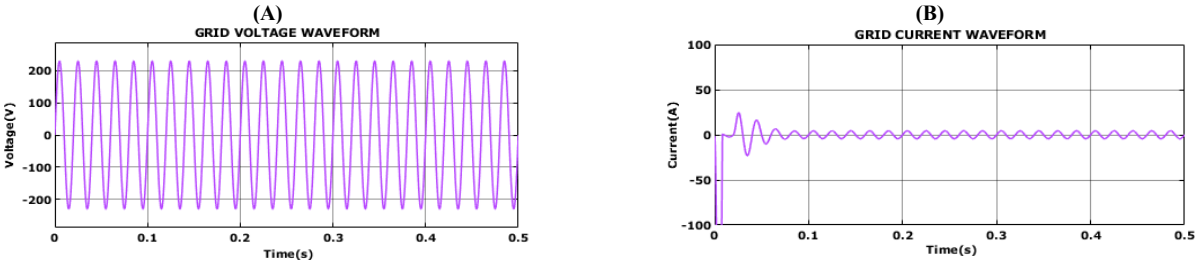

Fig. 13: Grid Voltage and Current Waveform.

In the following waveform, the grid voltage stabilizes at 210V, indicating a consistent and steady voltage level. Additionally, the current waveform shows a stable value of 5A, with no deviation, demonstrating this at 0.1S in Figure 13.

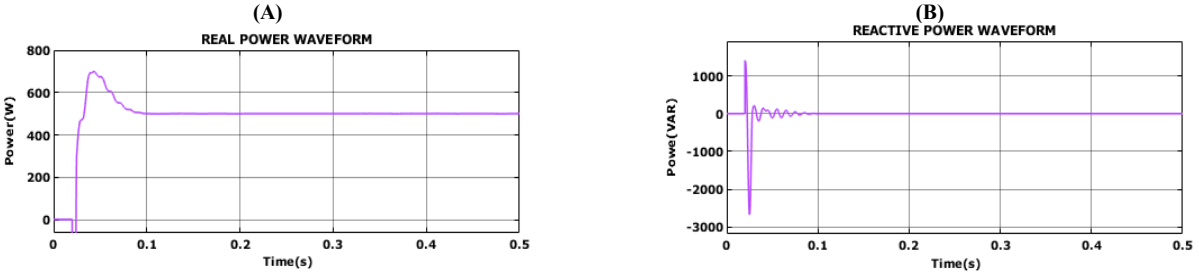

Fig. 14: Real and Reactive Power Waveform.

Figure 14 depicts the stabilization of real power at 500W, indicating a consistent and steady level of real power. Additionally, the reactive power remains continuously stabilized at zero, showing no reactive power response or fluctuation.

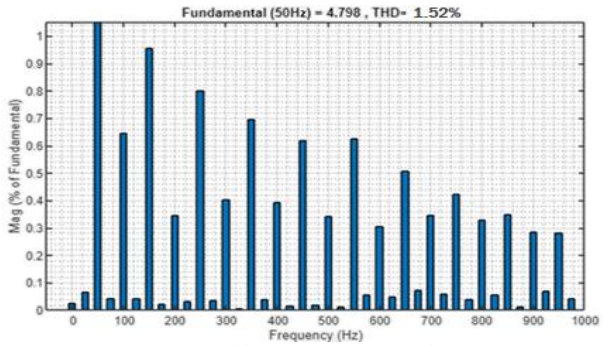

Fig. 15: Grid Current THD Waveform.

Total harmonic distortion (THD) in Figure 15 shows that there is harmonic distortion in the waveform value of 1.52%. In general, waveforms with more sinusoidal shapes tend to have lower THD values, reflecting a cleaner and more ideal electrical signal without significant distortion.

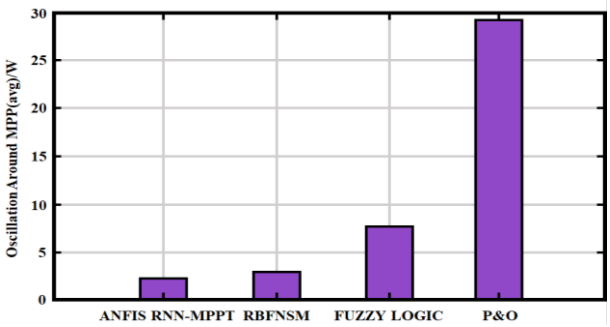

Fig. 16: Comparison of Oscillation Around MPP.

The fluctuation around MPP for both optional and current approaches is displayed in Figure 16. The fuzzy logic technique received 7.1 W, the RBFNSM received 5 W, the existing P&O techniques received 29 W, and 4 W were given to the proposed ANFISRNN-MPPT oscillation. Consequently, in contrast to the currently employed, our less oscillation was seen around MPP in the RNN-MPPT proposed algorithm.

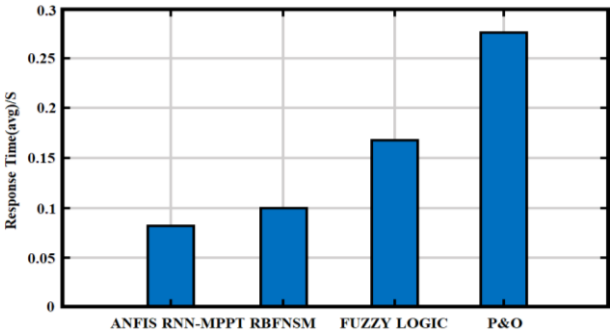

Fig. 17: Comparison of Response Time.

The response time, Figure 17, shows a comparison of the intended and present tactics. The P&O approach takes 0.28 seconds to respond. It takes 0.08 seconds for ANFIS RNN-MPPT, 0.17 seconds for fuzzy logic, and 0.1 seconds for RBFNSM. This indicates that our proposed ANFIS RNN-MPPT was given a speedier answer.

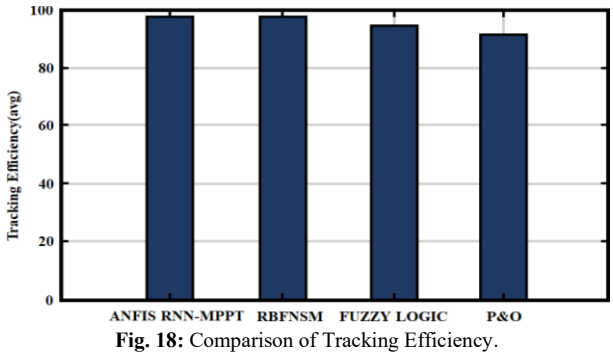

Fig. 18: Comparison of Tracking Efficiency.

Figure 18 shows the efficiency comparison of the planned and existing techniques. Our proposed ANFIS RNN-MPPT strategy has an efficiency of 99.52%, whereas the RBFNSM method, fuzzy logic method, and P&O method have efficiencies of 99.12%, 97.35%, and 95.14%, respectively. Our predicted effectiveness was superior to others.

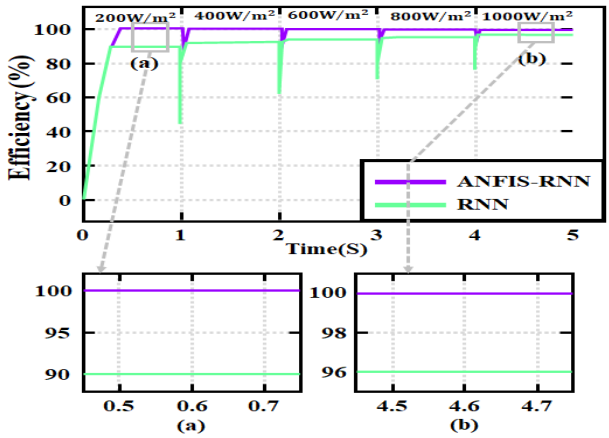

Fig. 19: Efficiency Comparison between Cascaded ANFIS-RNN MPPT and RNN MPPT.

As a function of irradiation step variation, Figure 19 shows the real-time MPPT efficiency of both RNN MPPT and ANFIS-RNN MPPT approaches. The impressive performance of the ANFIS-RNN MPPT, which maintains efficiency close to 100% even at lower irradiance levels of 200 W/m², demonstrates its strong tracking capabilities throughout irradiance levels. 96.7% at 1000 W/m² is the maximum efficiency that the standard RNN MPPT achieves, with a much lower efficiency, especially at lower irradiance levels. The ANFIS-RNN MPPT has the potential to provide dependable performance in a range of irradiance situations, as this comparison amply illustrates, as it tracks the genuine MPP with virtually flawless accuracy.

5. Conclusion

This paper presents a novel hybrid Cascaded ANFIS-RNN-based MPPT and boost converter system for Photovoltaic (PV)-tied grid systems. This system addresses the challenges posed by the nonlinear output power of solar modules due to varying atmospheric conditions. The proposed boost converter efficiently converts the variable DC voltage from PV panels into a stable and suitable voltage level for grid integration, ensuring high efficiency and low Total Harmonic Distortion (THD). Cascaded ANFIS-RNN-based MPPT technique accurately tracks the photovoltaic system's ideal power point, maximizing power generation. The cascaded ANFIS controller provides a robust and adaptive approach for MPP tracking, further enhanced by integrating an RNN into the ANFIS controller, improving tracking accuracy and convergence speed. A 1ϕVSI converts DC-AC supply for grid distribution, controlled by a PI controller. The proposed system, implemented in MATLAB/Simulink, demonstrates superior performance compared to existing topologies, highlighting its potential for enhancing power generation efficiency in PV-tied grid systems with existing topologies The proposed method's efficacy, demonstrating a THD value of 1.52% and superior performance in response time and tracking efficiency. The major limitation of this work is the lack of real-time validation, which must be carried out in future works, enabling the study of the real-time applicability of the proposed concept.

References

[1] Rahman S, Saha S, Islam SN, Arif MT, Mosadeghy M, Haque ME, Oo AM, “Analysis of power grid voltage stability with high penetration of solar PV systems,” IEEE Transactions on Industry Applications, Vol. 57, No. 3, (2021), pp. 2245-2257. https://doi.org/10.1109/TIA.2021.3066326.

[2] Kabir E, Kumar P, Kumar S, Adelodun AA, Kim KH, “Solar energy: Potential and prospects,” Renewable and Sustainable Energy Reviews, Vol. 82, (2018), pp. 894-900. https://doi.org/10.1016/j.rser.2017.09.094.

[3] Sandhiya S, Inbamani A, “Experimental analysis on different effects of PV module with respect to panel angle using machine learning algorithms information technology in industry”, Vol. 9, No. 3, (2021), pp. 367-374.

[4] Al-Shetwi AQ, Hannan MA, Jern KP, Alkahtani AA, Pg Abas AE, “Power quality assessment of grid-connected PV system in compliance with the recent integration requirements,” Electronics, Vol. 9, No. 2, (2020), pp. 366. https://doi.org/10.3390/electronics9020366.

[5] Subramaniam U, Vavilapalli S, Padmanaban S, Blaabjerg F, Holm-Nielsen JB, Almakhles D, “A hybrid PV-battery system for ON-grid and OFF-grid applications—Controller-in-loop simulation validation,” Energies, Vol. 13, No. 3, (2020), pp. 755. https://doi.org/10.3390/en13030755.

[6] Zhang G, Li Z, Zhang B, Halang WA, “Power electronics converters: Past, present and future,” Renewable and Sustainable Energy Reviews, Vol. 81, (2018), pp. 2028-2044. https://doi.org/10.1016/j.rser.2017.05.290.

[7] Raghavendra KV, Zeb K, Muthusamy A, Krishna TN, Prabhudeva Kumar SV, Kim DH, Kim MS, Cho HG, Kim HJ, “A comprehensive review of DC–DC converter topologies and modulation strategies with recent advances in solar photovoltaic systems,” Electronics, Vol. 9, No. 1, (2019), pp. 31. https://doi.org/10.3390/electronics9010031.

[8] Ibrahim SA, Nasr A, Enany MA, “Maximum power point tracking using ANFIS for a reconfigurable PV-based battery charger under non-uniform operating conditions,” IEEE Access, Vol. 9, (2021), pp. 114457-114467. https://doi.org/10.1109/ACCESS.2021.3103039.

[9] Mennai N, Medoued A, Soufi Y, "Comparative analysis of dynamic and steady State performances of Hill climbing and incremental conductance MPPT controllers for PV systems," Journal of Renewable Energy and Environment, Vol. 11, No. 3, (2024), pp. 35-41.

[10] Ali MN, Mahmoud K, Lehtonen M, Darwish MM, “An efficient fuzzy-logic based variable-step incremental conductance MPPT method for grid-connected PV systems,” IEEE Access, Vol. 9, (2021), pp. 26420-26430. https://doi.org/10.1109/ACCESS.2021.3058052.

[11] Malay I, Zakyla Akbar D, Arindra K, Al Hafiz F, Qirania Sakila N, Qadar Karo Karo S, Habib M, Simarmata T, “A Comparative Study of Photovoltaic Maximum Power Point Tracking Algorithms Under Dynamic Weather Conditions," International Journal of Society Reviews, Vol. 2, No. 10, (2025), pp. 1702-1717.

[12] Rajesh K, "Radial basis function neural network MPPT controller-based microgrid for hybrid stand-alone energy system used for irrigation," Circuit world, Vol. 49, No. 2, (2023), pp. 251-266. https://doi.org/10.1108/CW-03-2022-0076.

[13] Kumar AS, Ramesh S, Arukula P, Parveen MAS, “Analyzing PV power systems using MPPT based on Artificial Neural Networks," Nanotechnol. Percept, Vol. 20, (2024), pp. 792-797. https://doi.org/10.62441/nano-ntp.v20iS9.56.

[14] El Haji I, Megrini M, Kchikach M, Sahbani S, Gaga A, El Hasnaoui A, “Performance optimization of symmetrical multi-level boost converter using hybrid MPPT-ANN for solar energy applications," Results in Engineering, Vol. 26, (2025), pp. 104729. https://doi.org/10.1016/j.rineng.2025.104729.
[15] Bakare MS, Abdulkarim A, Nuhu Shuaibu A, Mustafa Muhamad M, “Enhancing solar power efficiency with hybrid GEP ANFIS MPPT under dynamic weather conditions," Scientific reports, Vol. 15, No. 1, (2025), pp. 5890. https://doi.org/10.1038/s41598-025-90417-1.
[16] Charaabi A, Barambones O, Zaidi A, Zanzouri N, “A novel two stage controller for a DC-DC boost converter to harvest maximum energy from the PV power generation,” In Actuators, Vol. 9, No. 2, (2020), pp. 29. https://doi.org/10.3390/act9020029.
[17] Rathnayake N, Rathnayake U, Dang TL, Hoshino Y, “A cascaded adaptive network-based fuzzy inference system for hydropower forecasting,” Sensors, Vol. 22, No. 8, (2022), pp. 2905. https://doi.org/10.3390/s22082905.
[18] Zaghba L, Borni A, Khennane Benbitour M, Fezzani A, Alwabli A, Bajaj M, Ahmad Dost Mohammadi S, Ghoneim SSM, “Enhancing grid-connected photovoltaic system performance with novel hybrid MPPT technique in variable atmospheric conditions," Scientific Reports, Vol. 14, No. 1, (2024): 8205. https://doi.org/10.1038/s41598-024-59024-4.
[19] Ghamari SM, Hajihosseini M, Habibi M, Aziz A, “Design of an adaptive robust PI controller for DC/dc boost converter using reinforcement-learning technique and snake optimization algorithm," IEEE Access, Vol. 12, (2024), pp. 141814-141829. https://doi.org/10.1109/ACCESS.2024.3440580.